substrate integrated waveguide (HMSIW) 3dB coupler, IEEE Microwave Wireless Compon Lett 17 (2007), 22–24.
7. E. Penard, and J.P. Daniel, Mutual coupling between microstrip antennas, Electron Lett 19 (1983), pp. 178–180.
8. C.F. Xie and W.J. Qiu, Antenna principle and technology, Xidian University Publishing House, Xian, China, 1991.
9. G.A. Kyriacou and J.N. Sahalos, An easy to use method to define the input impedance of a probe-fed rectangular microstrip antenna, Archiv Fiir Electrotechnik 70 (1987), pp. 349–357.
10. J. Venkataraman and D.C. Chang, Input impedance to a probe-fed rectangular microstrip patch antenna, Electromagnetics 3 (1983), 387–399.
11. G.A. Kyriacou and J.N. Sahalos, Analysis of a probe-fed short-circuited microstrip antenna, IEEE Trans Vehicular Technol 45 (1996), 427–430.
12. P. Bhartia, K.V.S. Rao, and R.S. Tomar, Millimeter-wave microstrip and printed circuit antennas, Artech House, Nonvood, MA, 1991.

A COMPACT CASCADE QUADRUPLET BANDPASS FILTER WITH LOW TEMPERATURE COFIRED CERAMIC TECHNOLOGY

Hong-Ching Lin,[1] Pang Lin,[1] Ching-Wen Tang,[2] and Sea-Fue Wang[3]
[1] Department of Materials Science and Engineering, National Chiao Tung University, Hsinchu, Taiwan, Republic of China
[2] Department of Communications Engineering, National Chung Cheng University Chiayi, Taiwan, Republic of China; Corresponding author: cwtang@ccu.edu.tw
[3] Department of Materials and Mineral Resources Engineering, National Taipei University of Technology, Taipei, Taiwan, Republic of China

Received 31 March 2008

ABSTRACT: *In this article, a compact cascade quadruplet bandpass filter has been proposed. This bandpass filter has been realized with the semilumped method and can generate a pair of transmission zeros at the two sides of passband by using the nonadjacent cross coupling. The analysis and design procedures are provided in this article. To miniaturize the size of the circuit and improve its performance, multilayered structure and the low-temperature cofired ceramic technology are employed to design and fabricate the filter. Measurement results agree well with the electromagnetic simulation, which can validate the proposed structure.* © 2008 Wiley Periodicals, Inc. Microwave Opt Technol Lett 50: 3218–3220, 2008; Published online in Wiley InterScience (www.interscience.wiley.com). DOI 10.1002/mop.23910

Key words: *bandpass filter; low-temperature cofired ceramic; compact filters*

1. INTRODUCTION

Compact size and low insertion loss are essential specifications within the modern telecommunication systems. To realize multiband behavior, RF transceivers with more bandwidth and flexibility are utilized. Meanwhile, the technologies for integrating passive circuits to achieve multifunction, high performance, and chip-size are attractive for the microwave and millimeter-wave applications. Therefore, the low-temperature cofired ceramic (LTCC) [1–6] seems to be one of the most efficient methods for miniaturizing and packaging technologies [7–10] because LTCC can integrate both passive and active components in a module to achieve the system-in-a-package (SiP) approach.

The bandpass filter is one of the most important components in the RF front-end. It can select passband frequencies and reduce the influence from frequencies of the adjacent channels. The lowpass prototypes have been discussed in several articles [11, 12]. Levy [13] has proposed a unified theory for the synthesis of exactly equiripple lowpass prototypes. To realize a single pair of attenuation poles at finite frequencies, Yu and Chang [14] and Hong and Lancaster [15] adopt the microstrip open-loop resonators. Hsu et al. [16] have also adopted the coupled-resonators to design the group-delay equalizers. In this article, the coupling scheme is proposed to control the locations of transmission zeros at both sides of passband skirts. Detailed analyses of coupling scheme and design equations are introduced in Section 2. The multilayered structure of bandpass filter and fabricated unit are provided in Section 3. Section 4 concludes this article.

2. THEORY OF FILTER

The immittance inverter is adopted to analyze our proposed filter [17, 18]. The four-ordered quasi-elliptic bandpass filter with cross-coupling can generate a first pair of transmission zeros at finite frequencies. As shown in Figure 1, the inverter J_{14} is connected to nodes A and B. The condition of generating the first pair of transmission zeros is $Y_{21\ \text{path ACDB}} + Y_{21\ \text{path AB}} = 0$. Assuming all of the resonators $B_i(\omega)$ are equal to $B(\omega)$, the equation can be derived as

$$\frac{J_{12}J_{23}J_{34}}{B^2(\omega) - J_{23}^2} = -J_{14} \tag{1}$$

Within the susceptance $B(\omega)$, both the inductor L and capacitor C are combined. This result may make the denominator of Eq. (1) greater than zero. Table 1 shows the relation between J_{12}, J_{23}, J_{34}, and J_{14}. The positive value of J-inverter represents the circuit using the inductive coupling for the feedback loop, and the negative value of J-inverter represents the circuit using the capacitive coupling for the feedback loop.

Using the combline filter as an example, the center frequency and bandwidth ratio are defined as 2.4 GHz and 0.1, respectively, and the characteristic impedance Z_0 and the electric length θ of transmission line are chosen as 25 Ω and 25°, respectively. If the ripple of Chebyshev response is 0.01 dB, then the values of each inverter, as shown in Figure 1, can be calculated as $J_{01} = J_{45} = 0.016$, $J_{12} = J_{34} = 0.00992$, and $J_{23} = 0.00729$. Here, the frequency of transmission zero is located at the lower side of the passband at 1.9 GHz, and J_{14} can be derived, by Eq. (1), as -0.000394. Figure 2 shows the simulated results of four-ordered bandpass filters with and without the cross-coupled inverter J_{14}. For simplification, the inverters can be replaced with quarter-

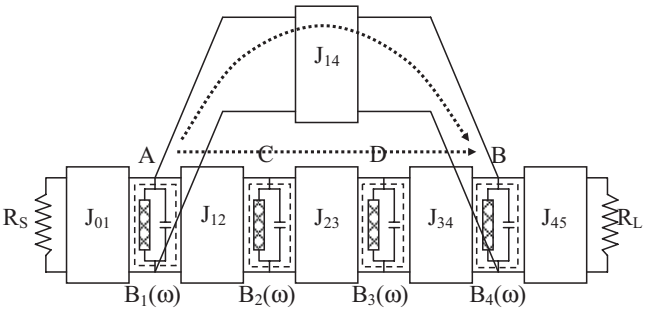

Figure 1 Equivalent circuit of four-ordered quasi-elliptic bandpass filter with cross coupling

TABLE 1 Conditions of Appearing the Transmission Zero

$J_{14} = +\pi/2$			$J_{14} = -\pi/2$		
J_{12}	J_{23}	J_{34}	J_{12}	J_{23}	J_{34}
$+\pi/2$	$+\pi/2$	$-\pi/2$	$-\pi/2$	$-\pi/2$	$+\pi/2$
$+\pi/2$	$-\pi/2$	$+\pi/2$	$-\pi/2$	$+\pi/2$	$-\pi/2$
$-\pi/2$	$+\pi/2$	$+\pi/2$	$+\pi/2$	$-\pi/2$	$-\pi/2$
$-\pi/2$	$-\pi/2$	$-\pi/2$	$+\pi/2$	$+\pi/2$	$+\pi/2$

wavelength transmission lines. It depicts that the two transmission zeros of the simulated filter with cross-coupling J_{14} are located at 1.93 and 2.97 GHz, respectively.

In Figure 2, the return loss of the filter with cross-coupling is less than the filter without cross-coupling. Moreover, the closer the two frequencies of transmission zeros to the center frequency, the worse is the return loss. If two admittances Y_i, at the inputs of inverter J_{01} and J_{45}, are modified, the performance of return loss can be improved as shown in Figure 3. The admittance Y_i is matched at the central frequency and can be derived as in (2), and two inverters J_{01} and J_{45} are also modified as (3) and (4). As a result, the two inverters J_{01} and J_{45} are revised as 0.01667. Figure 4 shows the simulated results of modified four-ordered quasi-elliptic bandpass filter and the original filter with cross-coupling J_{14}.

$$Y_i = \frac{J_{12}J_{34} - J_{23}J_{14}}{J_{23}} \tag{2}$$

$$J_{01} = \sqrt{\frac{J_{12}J_{34} - J_{23}J_{14}}{J_{23}R_S}} \tag{3}$$

$$J_{45} = \sqrt{\frac{J_{12}J_{34} - J_{23}J_{14}}{J_{23}R_L}} \tag{4}$$

3. FABRICATION AND MEASUREMENT

The cross-coupled four-ordered bandpass filter as an example. This filter is fabricated with the substrate of Dupont 951. Its dielectric constant and loss tangent are 7.8 and 0.0045, respectively. The 2.4-GHz LTCC filter is designed on four upper layers with the sheet of 1.57 mil, followed by six layers with the sheet of 3.6 mil, six layers with the sheet of 1.57 mil, and finally two layers with the sheet of 3.6 mil at the bottom. Its overall size is 132 mil × 92 mil × 41.4 mil. The simulation is carried out with the assistance of full-wave electromagnetic (EM) simulator, namely Sonnet from Sonnet Software. To improve the accuracy of measurement, the

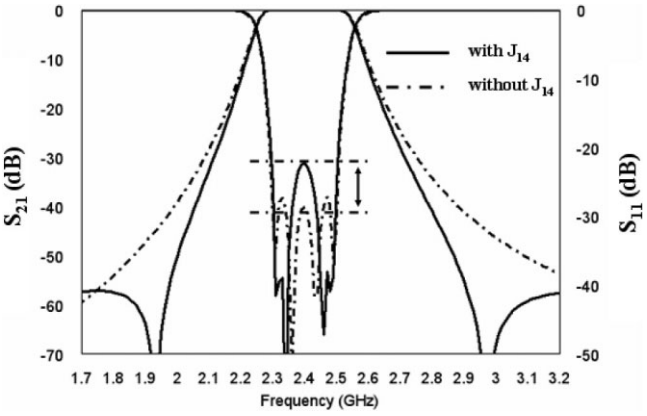

Figure 2 Simulated results of four-ordered bandpass filters.

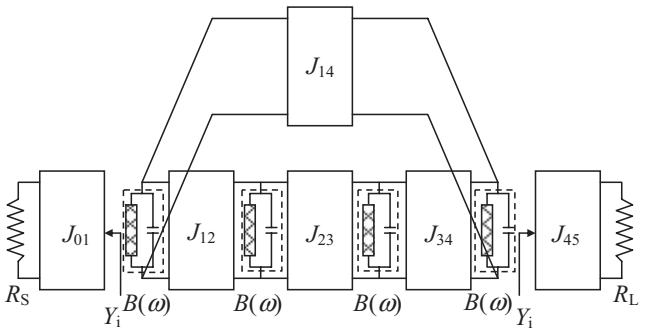

Figure 3 Four-ordered bandpass filter, which has considered the impedance matching in the inverters J_{01} and J_{45}

on-wafer tester has been chosen. The network analyzer, Agilent N5230A PNA_L, is used to measure, and the short-open-load-through (SOLT) is adopted for calibration. To design the cross-coupled bandpass filter, with multilayered structure, the semi-lumped method is suitable to realize four resonators. This semilumped method is composed of a transmission line section shunted with a capacitor. These capacitors within four resonators simply use the metal-insulator-metal (MIM) architecture to realize. The inductance coupling of L_{14} is realized by the edge coupling between the transmission lines of first and fourth resonators. The other inductance couplings of L_{12} and L_{34} adopt the broadside-coupled transmission lines. The capacitance coupling of C_{23} uses the MIM capacitor directly. Figure 5(a) reveals the detailed three-dimensional (3D) structure of 2.4-GHz LTCC bandpass filter.

As shown in Figure 5(b), the pair of frequencies of measured and EM simulated transmission zeros are 1.93, 3.1 GHz, and 1.9, 3 GHz, respectively. At the frequency of 2.4 GHz, the measured and EM simulated insertion losses are less than 3.3 and 3 dB, respectively, whereas the return losses are greater than 19.6 and 27.3 dB. At the neighboring of passband, the outband rejection is more than the level of 40 dB.

4. CONCLUSION

The LTCC bandpass filter with coupling scheme has been proposed in this article. The theory of generating the transmission

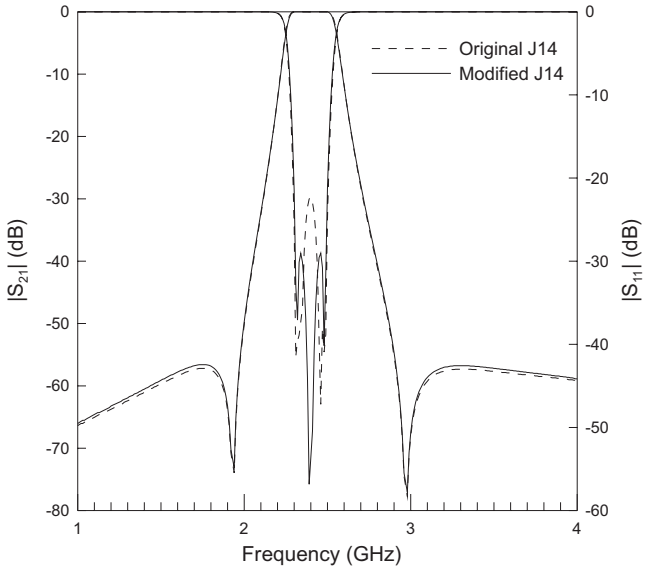

Figure 4 Compare the responses of modified four-ordered bandpass filter with the original filter with cross-coupling J_{14}

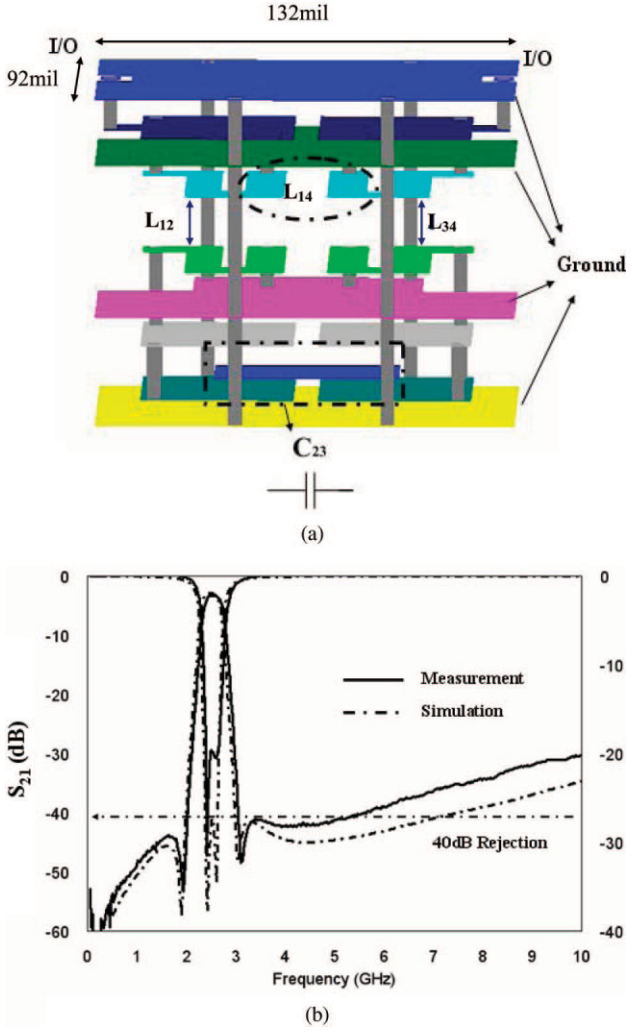

Figure 5 Fabricated cross-coupled four-ordered LTCC bandpass filter. (a) 3D structure and (b) measured and EM simulated results. [Color figure can be viewed in the online issue, which is available at www.interscience.wiley.com]

zeros and the design procedures of filters have been analyzed. The proposed bandpass filter fabricated with the multiayered structure is realized using the semilumped method. The fabricated bandpass filter with the characteristics of high integration and small size is very suitable for the implementation in the multichip module. Agreement between measurement and theoretical prediction has evidenced the feasibility of our study.

ACKNOWLEDGMENTS

This work was supported in part by the National Science Council, Taiwan, Republic of China, under grant NSC 96-2628-E-194-002-MY2.

REFERENCES

1. K. Kunihiro, S. Yamanouchi, T. Miyazaki, Y. Aoki, K. Ikuina, T. Ohtsuka, and H. Hida, A diplexer-matching dual-band power amplifier LTCC module for IEEE 802.11a/b/g wireless LANs, in Proceedings of IEEE Radio Frequency Integrated Circuits Symposium Digest, Fort Worth, TX, 2004, pp. 303–306.
2. J. Muller and H. Thust, 3D-intergration of passive RF-components in LTCC, in Proceedings of Pan Pacific Microelectronics Symposium Digest, 1997, pp. 211–216.
3. C.Q. Scrantom and J.C. Lawson, LTCC technology: Where we are and where we're going-II, in Proceedings of IEEE MTT-S International Microwave Symposium Digest, Anaheim, CA, 1999, pp. 193–200.
4. Y. Rong, K.A. Zaki, M. Hageman, D. Stevens, and J. Gipprich, Low temperature cofired ceramic (LTCC) ridge waveguide bandpass filters, in Proceedings of IEEE MTT-S International Microwave Symposium Digest, Anaheim, CA, 1999, pp. 1147–1150.
5. D. Heo, A. Sutono, E. Chen, Y. Suh, and J. Laskar, A 1.9 GHz DECT CMOS power amplifier with fully integrated multilayer LTCC passives, IEEE Microwave Wireless Components Lett 11 (2001), 249–251.
6. W.Y. Leung, K.K.M. Cheng, and K.L. Wu, Design and implementation of LTCC filters with enhanced stop-band characteristics for bluetooth applications, in Proceedings of Asia-Pacific Microwave Conference, 2001, Taipei, Taiwan, pp. 1008–1011.
7. Y.L. Low and R.C. Frye, The impact of miniaturization and passive component integration in emerging MCM applications, in Proceedings of IEEE Multi-Chip Module Conference (MCMC'97), 1997, pp. 27–32.
8. A.B. Frazier, R.O. Warringtun, and C. Friedrich, The miniaturization technologies: Past, present, and future, IEEE Trans Indus Elec 42 (1995), 423–430.
9. A. Matsuzawa, RF-SoC-Expectations and required conditions, IEEE Trans Microwave Theory Tech 50 (2002), 245–253.
10. K.L. Tai, System-in-package (SIP): Challenges and opportunities, in Proceedings of the Asia and South Pacific Design Automation Conference (ASP-DAC), 2000, pp. 211–216.
11. R.M. Kurzrok, General four-resonator filters at microwave frequencies, IEEE Trans Microwave Theory Tech 14 (1966), 295–296.
12. J.D. Rhodes, A low-pass prototype network for microwave linear phase filters, IEEE Trans Microwave Theory Tech 18 (1970), 290–301.
13. R. Levy, Filters with single transmission zeros at real or imaginary frequencies, IEEE Trans Microwave Theory Tech 24 (1976), 172–181.
14. C.C. Yu and K. Chang, Novel compact elliptic-function narrow-band bandpass filters using microstrip open-loop resonators with coupled and crossing lines, IEEE Trans Microwave Theory Tech 46 (1998), 952–958.
15. J.S. Hong and M.J. Lancaster, Design of highly selective microstrip bandpass filters with a single pair of attenuation poles at finite frequencies, IEEE Trans Microwave Theory Tech 48 (2000), 1098–1107.
16. H.T. Hsu, H.W. Yao, K.A. Zaki, and A.E. Atia, Synthesis of coupled-resonators group-delay equalizers, IEEE Trans Microwave Theory Tech 50 (2002), 1960–1968.
17. G.L. Matthaei, L. Young, and E.M. Jones, Microwave filters, impedance-matching network, and coupling structures, Artech House, Norwood, MA, 1980.
18. J.S.G. Hong and M.J. Lancaster, Microstrip filters for RF/microwave applications, Wiley, New York, NY, 2001.

TIME INTERVAL MEASUREMENT FOR RESONATOR FIBER OPTIC GYROSCOPE BASED ON SLOW LIGHT TECHNOLOGY

Ying Li and Xinglin Chen
Department of Control Science and Engineering, Harbin Institute of Technology, Harbin 150001, China; Corresponding author: liyinghit@gmail.com

Received 4 April 2008

ABSTRACT: *It is noted that the high-group dispersion leads to huge enhancement of the fiber optic gyroscope's sensitivity in a resonating structure, and an approach to evaluate and design resonator gyroscope with slow-light property is proposed. And then we could adopt time in-*